Biochimie 95 (2013) 2365–2375

Contents lists available at ScienceDirect

Biochimie

journal homepage: www.elsevier.com/locate/biochi

Research paper

Biochemical, functional, structural and phylogenetic studies on Intercro, a new isoform phospholipase A_2 from *Crotalus durissus terrificus* snake venom

Lara F. Vieira [a, 1], Angelo J. Magro [b, 1], Carlos A.H. Fernandes [b, 1], Bibiana M. de Souza [c], Walter L.G. Cavalcante [b, d], Mário S. Palma [c], José C. Rosa [e], André L. Fuly [f], Marcos R.M. Fontes [b], Márcia Gallacci [d], Diana S. Butzke [g, h], Leonardo A. Calderon [g], Rodrigo G. Stábeli [g], José R. Giglio [a, *], Andreimar M. Soares [g, *]

[a] *Departamento de Bioquímica e Imunologia, FMRP – USP, Ribeirão Preto, SP, Brazil*
[b] *Departamento de Física e Biofísica, Instituto de Biociências, UNESP, Botucatu, SP, Brazil*
[c] *Instituto de Biociências, UNESP, Rio Claro, SP, Brazil*
[d] *Departamento de Farmacologia, Instituto de Biociências, UNESP, Botucatu, SP, Brazil*
[e] *Centro de Química de Proteínas, USP, Ribeirão Preto, SP, Brazil*
[f] *Departamento de Biologia Molecular e Celular, UFF, Niterói, RJ, Brazil*
[g] *Centro de Estudos de Biomoléculas Aplicadas à Saúde, CEBio, Fundação Oswaldo Cruz, FIOCRUZ Rondônia e Departamento de Medicina, UNIR, Porto Velho 76812-245, RO, Brazil*
[h] *Faculdade São Lucas, Porto Velho, RO, Brazil*

ARTICLE INFO

Article history:
Received 10 July 2012
Accepted 25 August 2013
Available online 11 September 2013

Keywords:
Intercro
CB isoforms
Phospholipase A_2
Oligomerization
Crotalus durissus terrificus

ABSTRACT

Crotoxin is a neurotoxin from *Crotalus durissus terrificus* venom that shows immunomodulatory, anti-inflammatory, antimicrobial, antitumor and analgesic activities. Structurally, this toxin is a heterodimeric complex composed by a toxic basic PLA_2 (Crotoxin B or CB) non-covalently linked to an atoxic non-enzymatic and acidic component (Crotapotin, Crotoxin A or CA). Several CA and CB isoforms have been isolated and characterized, showing that the crotoxin venom fraction is, in fact, a mixture of different molecules derived from the combination of distinct subunit isoforms. Intercro (IC) is a protein from the same snake venom which presents high similarity in primary structure to CB, indicating that it could be an another isoform of this toxin. In this work, we compare IC to the crotoxin complex (CA/CB) and/or CB in order to understand its functional aspects. The experiments with IC revealed that it is a new toxin with different biological activities from CB, keeping its catalytic activity but presenting low myotoxicity and absence of neurotoxic activity. The results also indicated that IC is structurally similar to CB isoforms, but probably it is not able to form a neurotoxic active complex with crotoxin A as observed for CB. Moreover, structural and phylogenetic data suggest that IC is a new toxin with possible toxic effects not related to the typical CB neurotoxin.

1. Introduction

Snake venoms are complex mixtures of bioactive compounds, especially proteins and peptides, which serve as weapons for defense and prey capture [1]. Human envenoming caused by snakebite accidents is very common in tropical and subtropical regions worldwide, causing a great impact on public health in developing countries [2]. On the other hand, snake venoms constitute a natural biological source of molecules, which have potential therapeutic value due to their high affinity and specificity for critical targets in cell and tissue organization [3,4].

Snake venom PLA_2s (svPLA_2s) enzymes/toxins are abundant in viperid snake venoms, displaying a large array of toxic effects as neurotoxicity, myotoxicity, cardiotoxicity, cytotoxicity, and impair effects in blood coagulation and platelet aggregation [5–9]. Part of these actions is attributed to the enzymatic activity of catalytically active svPLA_2s. However, the presence of some of these toxins without measurable enzymatic activity [1] evidences the presence of other toxic sites.

* Corresponding authors. Fax: +55 1636024725.
E-mail addresses: jrgiglio@fmrp.usp.br (J.R. Giglio), andreimar@fiocruz.br, andreims@hotmail.com (A.M. Soares).
[1] These authors contributed equally to the work.

0300-9084/$ – see front matter © 2013 Elsevier Masson SAS. All rights reserved.
http://dx.doi.org/10.1016/j.biochi.2013.08.028

One of the most interesting and studied svPLA$_2$s is found in crotoxin, a neurotoxin found in the *Crotalus durissus terrificus* venom [10] which has been implicated in immunomodulatory, anti-inflammatory, antimicrobial, antitumor and analgesic actions [11]. Structurally, this toxin is a heterodimeric complex composed by a toxic basic PLA$_2$ (crotoxin B or CB) non-covalently linked to an atoxic non-enzymatic and acidic component (crotapotin, crotoxin A or CA) [12,13]. Several isoforms of both subunits of crotoxin have been isolated and characterized [14], showing that the crotoxin venom fraction is, in fact, a mixture of different molecules derived from the combination of distinct subunit isoforms [14,15]. In 1975, Laure [16] observed the presence of a new protein named Intercro (IC), which is eluted between the crotamine and crotoxin chromatographic peaks, suggesting that this molecule is not associated to the CA subunit in the *C. durissus terrificus* venom.

In this work, we describe, for the first time, the biochemical characterization of IC and also performed functional and structural studies in order to compare this molecule with the crotoxin complex (CA/CB) and/or CB and get insights into its biological aspects. The results of these analyses indicated that IC is similar to CB isoforms. However, it is possible that IC could be a CA-independent new toxin evolved in toxic functions not related to the typical CB neurotoxic effects.

2. Material and methods

2.1. IC isolation

C. durissus terrificus venom was obtained from the Serpentarium of the University of São Paulo at Ribeirão Preto School of Medicine, located in the city of Ribeirão Preto, Brazil. One gram of the dry venom was dispersed in 5 mL of 0.05 M ammonium formate buffer (NH_4Fo) pH 3.5, and centrifuged at 755× *g* for 10 min at room temperature (~25 °C). The clear supernatant was then applied to a Sephadex G-75 column (4.5 cm × 132 cm) equilibrated with the same buffer. The elution was performed at a flow rate of 30 mL/h. Fractions of 10 mL/tube were collected and monitored at $\lambda = 280$ nm using an automatic fraction collector. The fractions were then lyophilized and stored at freezer. The fraction identified as Intercro (IC), which was located between crotoxin and crotamine fractions, was redissolved in the same buffer and then chromatographed in the same conditions. The principal peak was harvested, lyophilized and then dissolved in 1 mL of 0.1 M NH_4Fo, pH 3.5, and applied to a CM-Cellulose column (2.5 cm × 10 cm) previously equilibrated with this same buffer. The sample was eluted using a linear gradient (0.1–0.2 M NH_4Fo) at a flow rate of 20 mL/h, and fraction of 5 mL/tube was collected.

The sample was checked for purity by RP-HPLC using a 4.6 mm × 100 mm of a C18 column (4.6 mm × 100 mm) (Shimadzu), previously equilibrated with solvent A (5%, v/v, acetonitrile + 0.1%, v/v, trifluoroacetic acid) and then eluted with a gradient of solvent B (60%, v/v, acetonitrile + 0.1%, v/v, trifluoroacetic acid) from 0 to 100%, flow rate = 1.0 mL min^{-1}, during 110 min. Elution was carried out at room temperature (25 °C) and fractions were monitored at $\lambda = 280$ nm.

2.2. Protein estimation

The protein content of the crude venom or fractions was estimated by the micro biuret method as described by Itzhaki and Gil [17]. The standard curve was drawn with bovine serum albumin, using an extinction coefficient of 0.660 for 1.0 mg mL^{-1} at $\lambda = 280$ nm [18].

2.3. Biochemical characterization

2.3.1. Electrophoresis and mass spectroscopy

Determination of M_r was performed by means of SDS-PAGE according to Laemmli [19], both in the presence and absence of reducing agents. IC was then analyzed in a mass spectrometer, triple quadruple electrospray type (Quatmtro II, Micromass, Manchester, UK) using a nanoflow electrospray origin containing a fused silica capillary of 20 μm internal diameter, at 2.8 kvolts and 100 °C. The sample was introduced by means of a syringe type pump (Harvard, Inc. USA), at a flow rate of 300 nL min^{-1}, the mass spectra were collected as scan media (15–30 scans) and processed with MassLynx v.33 software (Micromass, Manchester, UK).

2.3.2. Primary structure

N-Terminal sequence of IC was carried out by means of an automatic protein microsequenator (Shimadzu PPSQ-21), based on Edman degradation. Automated protein sequencing was performed using peptides generated by digestion of IC with trypsin (proteomics grade, Promega) and chymotrypsin (Sigma Chem. Co., USA) in the proportion of 386 pmoles IC/20 pmoles digestive enzyme. Proteolytic fragments were submitted to RP-HPLC using a Nucleosil C18 column, (10 × 250 mm; 5 μm) (Wakosil, Japan), previously equilibrated with solvent A (5%, v/v, acetonitrile + 0.1%, v/v, trifluoroacetic acid), and then eluted with a concentration gradient of solvent B (80%, v/v, acetonitrile + 0.1%, v/v, trifluoroacetic acid) from 0 to 100%, flow rate = 1.5 mL min^{-1}, during 90 min, at 28 °C, monitored at $\lambda = 214$ nm. Peptides fractions were individually collected, pooled and concentrated using a speed-vac system; each tryptic/chymotryptic peptide was individually submitted to amino acid sequencing as reported above.

2.4. Functional characterization

2.4.1. PLA$_2$ activity upon egg yolk

The radial indirect hemolysis method was used, as described by Gutiérrez et al. [20], with a single modification, in which agar, instead of agarose, was employed. Gels containing the samples were incubated at 37 °C for 12 h. PLA$_2$ activity was measured through formation of translucid halos around the points of sample. Halos were then measured (in mm) for quantification of PLA$_2$ activity.

2.4.2. Upon fluorescent lipids

Acyl-NBD was used as substrate [21], final volume = 3.0 mL, in a Hitachi F450 fluorescence spectrophotometer at room temperature. Excitation and emission wavelengths were adjusted to 460 nm and 543 nm, respectively. The standard solution contained 50 mM Tris–HCl and 1 mM $CaCl_2$, pH 7.5. A previous reading A1 of absorbance during 2 min was taken with all components, except the enzyme. Then, the enzymatic activity was started by addition of the PLA$_2$, thus giving a second reading A2. Reaction was monitored during 12 min. The readings differences A2–A1 were so determined. The influence of cations was investigated in 50 mM Tris–HCl, pH 7.5, replacing Ca^{2+} by Ba^{2+}, Cu^{2+}, Fe^{2+}, Mg^{2+}, Mn^{2+} and Zn^{2+}, always at a final concentration = 5 mM. For the experiments carried out in the absence of Ca^{2+}, 10 mM EDTA was used. The effect of pH was also evaluated, using different buffers, at pH 3.5 to 12.5.

2.4.3. Neuromuscular blockade

Male Swiss mice were euthanized by exsanguination after cervical dislocation. The phrenic nerve-diaphragm preparations were removed and mounted vertically in a conventional isolated organ-bath chamber containing 15 mL of physiological solution of the following composition (mmol/l): NaCl, 135; KCl, 5; $MgCl_2$, 1; $CaCl_2$, 2; $NaHCO_3$, 15; Na_2HPO_4, 1; glucose, 11. This solution was continuously

gasified with 95% O_2 and 5% CO_2. The preparation was attached to an isometric force transducer (Grass, FT03) coupled to a signal amplifier (Gould Systems, 13-6615-50). Indirect contractions were evoked by supramaximal strength pulses (0.2 Hz; 0.5 ms; 3 V), delivered by an electronic stimulator (Grass S88K) and applied on the phrenic nerve by a suction electrode. The results were recorded on a computer through a data acquisition system (Gould Systems, Summit ACQuire and Summit DataViewer). The preparation was stabilized for at least 45 min before the addition of the following components: crotoxin complex (CA/CB) (10 μg mL^{-1}), CB (10 μg mL^{-1}), CA (10 μg mL^{-1}) and IC (10 μg mL^{-1}). In some experiments, 5 μg $mL^{-1}$of CA were added 45 min after CB (10 μg mL^{-1}) or IC 10 (μg mL^{-1}). The amplitudes of indirect twitches were measured during 90 min.

2.4.4. Myotoxic activity

Groups of 5 male Swiss mice (18–25 g) were i.m. injected with two doses (25 μg and 50 μg) of CB, IC and synthetic peptides dissolved in 50 μL of PBS. Controls received only PBS and, 3 h later, the blood was collected from the tail in heparinized capillaries and immediately centrifuged. Creatine kinase (CK) activity was evaluated using 4 μL of plasma and the kinetic kit CK-UV (Bioclin, Brazil). The plasma was incubated with reactant as recommended for 3 min at 37 °C and the reaction monitored at A_{340nm} during 3 min as recommended by kit manufacturer. CK activity was expressed in U/L, one unit being defined as the result of phosphorylation of one nmol of creatine/min [22].

2.4.5. Edema induction

Groups of 5 male Swiss mice (18–25 g) were i.d. injected in the subplantar region of the right paw with 50 μL of IC solution in PBS, after a previous evaluation of the paw volumes (zero time). The paws were measured at 30 min, 1 h and 3 h, always subtracting the volume at zero time. This measure was performed with a low-pressure pachymeter (Mytutoyo, Japan) and expressed as a % of induced edema [22].

2.4.6. IC chemical modification

Three milligram of IC was dissolved in 1.0 mL of 0.1 M NH_4HCO_3, pH 7.0 containing 0.7 mM EDTA. Then, 150 μL of a 0.8 mg mL^{-1} solution of *p*-bromophenacyl bromide (*p*-BPB) in ethanol were added followed by 24 h of incubation at room temperature [22]. Excess reactant was then removed by means of an AMICON YM-3 system, through successive washings with 0.05 M NH_4HCO_3, pH 8.0.

2.4.7. Analysis of results

The results obtained were expressed as mean ± standard deviations (SD) and statistically analyzed using the *t*-student test with the significance levels considered between $0.1 < p < 0.05$, with a confidence interval of 95%.

2.5. Structural and phylogenetic characterization

2.5.1. Dynamic light scattering experiments

Dynamic light scattering (DLS) measurements were performed with native IC in 20 mM Tris–HCl pH 7.0 at 10 °C (283 K) and 25 °C (298 K) with a protein concentration of 3.0 mg mL^{-1} using a DynaPro TITAN equipment (Wyatt Technology). For that, 100 measurements were carried out at each temperature condition and the results were analyzed using the program Dynamics v.6.10.

2.5.2. Alignment and phylogenetic analysis

IC homologous sequences selected for sequence alignment and phylogenetic analysis were obtained from NCBI (The National Center for Biotechnology Information) database using the BLASTP algorithm and BLOSUM62 substitution matrix. The minimum *e*-value presented by the selected sequences was $8e^{-113}$. Multiple sequence alignment was executed with the program AMAP v.2.2 [23] and the phylogenetic tree was build based on the Bayesian method MCMC (Monte Carlo-Markov chain), using the program MrBayes v.3.1.2 [24,25]. Two concurrent Markov Chain Monte Carlo (MCMC) runs of 3,000,000 generations were performed using four progressively heated chains, a heating parameter of 0.2, tree sampling every 1000 generations and a burn-in setting of 250 trees. The hypothetical phospholipase A_2 LOCI100145401 from *Xenopus tropicalis* was defined as out-group. All the IC-homologous sequences used in this study and their respective identification codes are shown in Table 1.

2.5.3. IC modeling and molecular dynamics simulation

Using the HHpred server based alignment [26] (score = 335.27; sequence identity = 98.0%), the crystallographic model of crotoxin B (isoform CB2/CBa_2) from *C. durissus terrificus* venom [27] (PDB ID 2qog_chain A) was selected as the ideal template in order to obtain the theoretical IC structure using program Modeller v.9.10 [28]. Thus, 10 models were initially generated and refined using the variable target function method (VTFM) with conjugate gradients (CG) and molecular dynamics (MD) with simulated annealing (SA). The best theoretical IC model was chosen according to stereochemical and energetic parameters calculated, respectively, with the programs MolProbity [29] and ProSA-web [30]. Following this step, the chosen initial theoretical IC model was submitted to MD simulations using the program GROMACS (Groningen Machine for Chemical Simulation) v.4.5.3 [31,32]. All simulations were executed in the presence of explicit water molecules [33] using an Ubuntu 9.04 Linux operational system and eight threads of a dual processor and quad-core Intel Xeon E5520 CPU (2.27 GHz) with 24 GB of RAM.

Table 1
Amino acid sequences of IC homologous proteins.

Protein (identification code)	Animal species/subspecies	GI code[a]
Protein sequences from snake venoms		
N6 basic phospholipase A_2 (Bsch)	*Bothriechis schlegelii*	38230125
N6 basic phospholipase A_2 (Cgod)	*Cerrophidion godmani*	38230123
Phospholipase A_2 3 (Ca3)	*Crotalus adamanteus*	387014170[b]
Phospholipase A_2, basic 9 (Cdc9)	*Crotalus durissus cumanensis*	313471401
Phospholipase A_2, basic 10 (Cdc10)	*Crotalus durissus cumanensis*	313471402
Phospholipase A_2 F6a (CdcF6)	*Crotalus durissus collilineatus*	239977500
Phospholipase A_2 Cdr-12 (Cdr12)	*Crotalus durissus ruruima*	239977492
Phospholipase A_2 Cdr-13 (Cdr13)	*Crotalus durissus ruruima*	239977493
Phospholipase A_2 F15 (CdtF15)	*Crotalus durissus terrificus*	239977494
Phospholipase A_2 F16 (CdtF16)	*Crotalus durissus terrificus*	239977495
Phospholipase A_2 F17 (CdtF17)	*Crotalus durissus terrificus*	239977496
Crotoxin CBa_2 (Cba_2)	*Crotalus durissus terrificus*	129470
Crotoxin CBb (Cbb)	*Crotalus durissus terrificus*	[c]
Crotoxin CBc (Cbc)	*Crotalus durissus terrificus*	48429036
Basic phospholipase A_2 Cvv-N6 (CvvN6)	Crotalus viridis viridis	82092667
Phospholipase A_2, basic isoform (Dacu)	*Deinagkistrodon acutus*	97180272
Phospholipase A_2 (Ghal)	*Gloydius halys*	2460027
Phospholipase A_2 trimucrotoxin (Pmuc1)	*Protobothrops mucrosquamatus*	26006835
TM-N49 (Pmuc2)	*Protobothrops mucrosquamatus*	77021843
N6b basic phospholipase A_2 (Scat)	*Sistrurus catenatus tergeminus*	38230127
N6 basic phospholipase A_2 (Smil)	*Sistrurus miliarius streckeri*	38230121
Phospholipase A_2 (Tfla)	*Trimeresurus flavoviridis*	28202237
Protein sequence from *Xenopus* genus (outgroup sequence)		
LOC100145401 protein (Xtrop)	*Xenopus tropicalis*	170285093

[a] Number identification code of the protein sequences in the NCBI data bank.
[b] Amino acid sequence determined by TSA (Transcriptome Shotgun Assembly).
[c] Amino acid sequence deduced from electron density map of CBb/CBa_2 crotoxin complex crystallographic structure (PDB ID 1OQS) (Faure et al., 2011).

The GROMOS 96 53a6 force field [34] was selected to perform the MD simulations and the protonation states of the charged groups were set to pH 7.0. The minimum distance between any atom in the models and the box wall was 1.0 nm. An energy minimization (EM) using a steepest descent algorithm was performed to generate the starting configuration of the systems. After this step, 200 ps of MD simulations with position restraints applied to the protein (PRMD) were executed in order to relax the systems gently. Further 35 ns of unrestrained MD simulations were calculated in order to evaluate the stability of the structures. All MD simulations were carried out in a periodic truncated cubic box under constant temperature (298 K) and pressure (1.0 bar), which were held constant by coupling to an isotropic pressure and external heat bath [35]. The overall structural quality of the theoretical IC structural model obtained after MD simulation was also checked with the programs MolProbity and ProSA-web.

3. Results

3.1. IC isolation and sequencing

The chromatographic profile obtained by gel filtration on Sephadex G-75 (Fig. 1) shows six main peaks, namely as: convulxin, gyroxin, crotoxin, Intercro (IC), crotamine and smaller peptides. The peak containing IC was then applied on the same column under the same conditions (Fig. 1B), resulting in one peak, which was further subject to an ion-exchange chromatography (Fig. 1C). At this step, the fraction III was identified as IC. The SDS-PAGE analysis under reducing conditions revealed a single polypeptide with M_r of 14 kDa (Fig. 1C, lane 5). However, three electrophoretic bands were seen when SDS-PAGE is performed in the absence of reducing agent (Fig. 1C, lane 3). The mass spectrometry analysis of dissociated CB subunit [36] purified by a rapid procedure described by Soares et al. [36] shown a M_r value of 14,246 (Fig. 2A), while free IC shown two peaks with M_r values of 14,188 and 14,284 (Fig. 2B), which could correspond to two predominant IC isoforms. The presence of svPLA$_2$ isoforms belonging the *Crotalus* genus is a common feature and is well described in scientific literature [37,38]. The complete amino acid sequence of IC is shown in Fig. 3 and its sequential identity with other svPLA$_2$s in Fig. 4. As attested by highly conserved residues involved in disulfides bridges and present in the catalytic site ($D_{42}XCCXXHD_{49}$) and Ca^{2+} binding site ($X_{27}CGXGG_{32}$), IC could be classified as member of the PLA$_2$s group II [39].

3.2. Biochemical and functional characterization

CB and IC showed PLA$_2$ activity upon egg yolk at doses of 5 μg (Fig. 5), but CB was the most active (Fig. 5A). As seen in Fig. 5A, pBPB

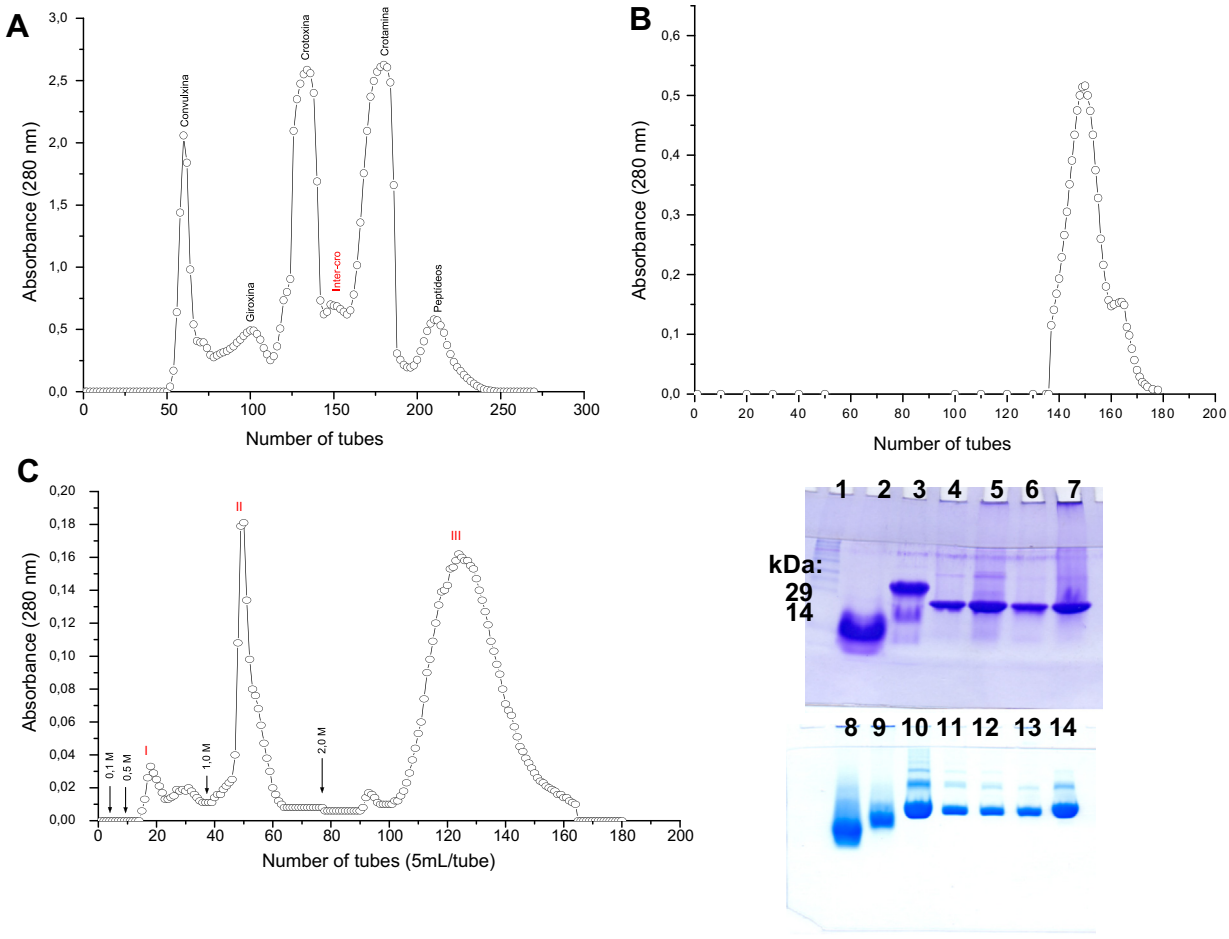

Fig. 1. (A) Gel filtration at room temperature, on Sephadex G-75, of 1 g of *C. durissus terrificus* snake venom. Crude fractions were identified as: convulxin, giroxin, crotoxin, Intercro (IC), crotamine, and smaller peptides. The sample was eluted with 0.05 M, pH 3.5 NH_4Fo buffer, at a flow rate of 30 mL/h, collecting 10 mL/tube; (B) second gel filtration chromatography of 90 mg of crude IC using the same column, under the same conditions, collecting 5 mL/tube; (C) ion-exchange chromatography of 33 mg of semi purified IC crude fraction using a CM-Cellulose with a linear concentration gradient of 0.1 M–0.2 M NH_4Fo, pH 3.5, at a flow rate of 20 mL/h, collecting 5 mL/tube. Fractions obtained were named I, II, and III. Insert: SDS-PAGE at 13.5% (w/v) acrylamide. Lanes 1–7 (with reducing agent): 1 – molecular weight; 2 – crotapotin; 3 – CTX; 4 and 5 – Intercro (gel filtration); 6 – Intercro (Fraction III CM-Cellulose); 7 – CB. Lanes 8–14 (absence of reducing agent): 8 – crotapotin (Fraction I-CM-Cellulose); 9 – Fraction II (CM-Cellulose); 10 – Intercro (Fraction III-CM-Cellulose); 11, 12, 13 and14-CB.

inhibited PLA_2 enzymatic activity. Moreover, PLA_2 enzymatic activity of fractions was assayed using different fluorescent phospholipids (NBD-PC, NDB-PG, NDB-PA and NDB-PE) (Fig. 5B). NBD-PC was the best substrate for both enzymes, being CB the most active enzyme again (Fig. 5B). The optimal pH value for PLA_2 activity was around 9 for CB and IC (Fig. 5C). The influence of metal ions (Ca^{+2}, Mg^{+2}, Zn^{+2}, Cu^{+2}, Mn^{+2}, Fe^{+2}, Ba^{+2}) was analyzed (Fig. 5D). Ca^{2+} and Mg^{2+} ions increased PLA_2 activity, which wasn't observed for the other ions tested.

IC (10 μg mL^{-1}) did not affect the amplitude of indirectly evoked twitches within 90 min of contact with mice phrenic-diaphragm preparation (Fig. 6). This finding contrasts with those observed for both crotoxin complex (CA/CB) (10 μg mL^{-1}), which induced a progressive depression of the twitch tension until complete block developed, and CB (10 μg mL^{-1}), which caused a slight but significant blockade of twitches from 45 min onwards. As shown in Fig. 6B, when CA (5 μg mL^{-1}) was added to the organ bath 45 min after IC (10 μg mL^{-1}) there was a discrete facilitation of twitch amplitude. This effect is in opposition to the synergism of the neuromuscular blockade observed when CA (5 μg mL^{-1}) was added after CB (10 μg mL^{-1}). CA (10 μg mL^{-1}) did not alter the amplitude of twitches. Regarding to myotoxic activity, we observed that CB was also more active than IC (Fig. 7A). Induced paw edema reached the maximum 30 min after injection (Fig. 7B).

3.3. Structural studies

Dynamic light scattering (DLS) experiments performed with native IC in 20 mM Tris–HCl, pH 7.0, at 10 °C (283 K) revealed a unimodal molecular distribution (Pd = 9.2%; 99.8% mass) with an average M_r around 16,000, as calculated from a hydrodynamic radius (R_H) value of 2.1 nm. However, DLS measurements carried out at 25 °C (298 K) indicated the occurrence of dimerization, which was observed by a broader unimodal molecular distribution

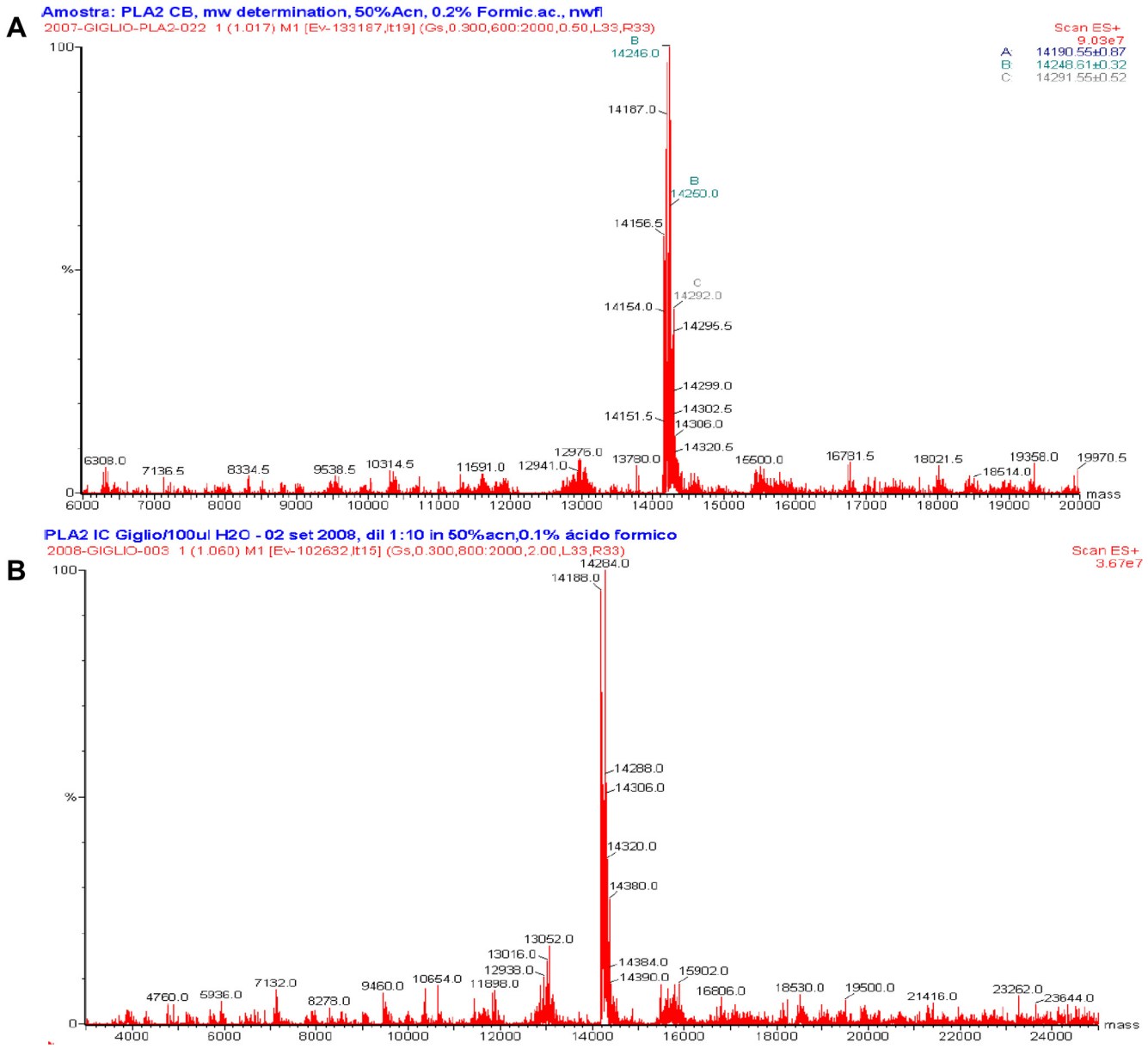

Fig. 2. Mass spectrometry of (A) CB and (B) IC isoforms in a quadrupole electrospray apparatus. The sample was introduced by means of a syringe type pump, at a flow rate of 300 nL min^{-1}, the mass spectra were collected as scan media (15–30 scans) and processed with MassLynx v.33 software.

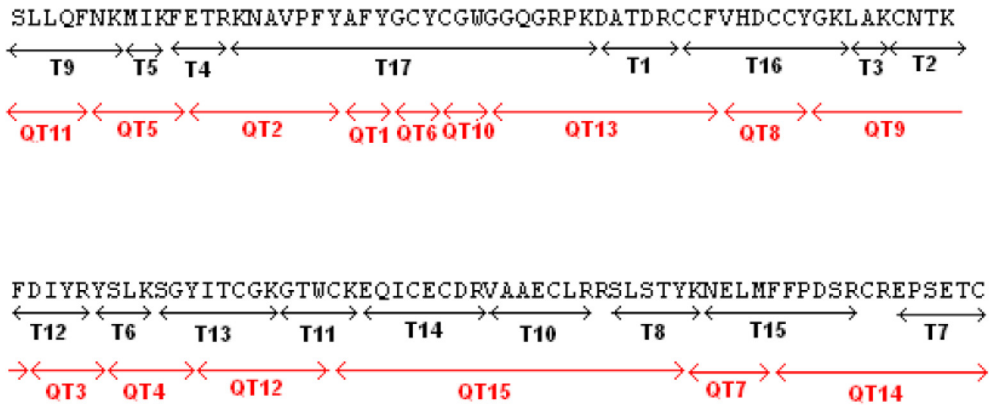

Fig. 3. Superposition of the amino acid sequences from tryptic and chymotryptic digestion resulting in the complete IC sequence.

(*Pd* = 17.3%; 99.3% mass) with an average M_r around 31,000, as calculated from a hydrodynamic radius (R_H) value of 2.6 nm.

As depicted in Fig. 8, the theoretical IC model after MD simulation keeps the same structural architecture and secondary elements of the chosen template [27] and other group II PLA_2s [37], presenting seven disulfide bonds, an N-terminal α-helix (h1), a Ca^{+2}-binding loop, two antiparallel α-helices (h2 and h3), a two-stranded antiparallel-sheet (β-wing), and a long C-terminal loop. Additionally, the overall structural quality of the MD model could be considered acceptable, because 95% of its residues were allocated in the allowed regions of the Ramachandran plot [29] and the *Z*-score is −5.08 [30]. A more detailed analysis of the MD simulation also supports the probable adequate stability of the model: between 10 ns and 35 ns, the amplitude of the backbone atoms

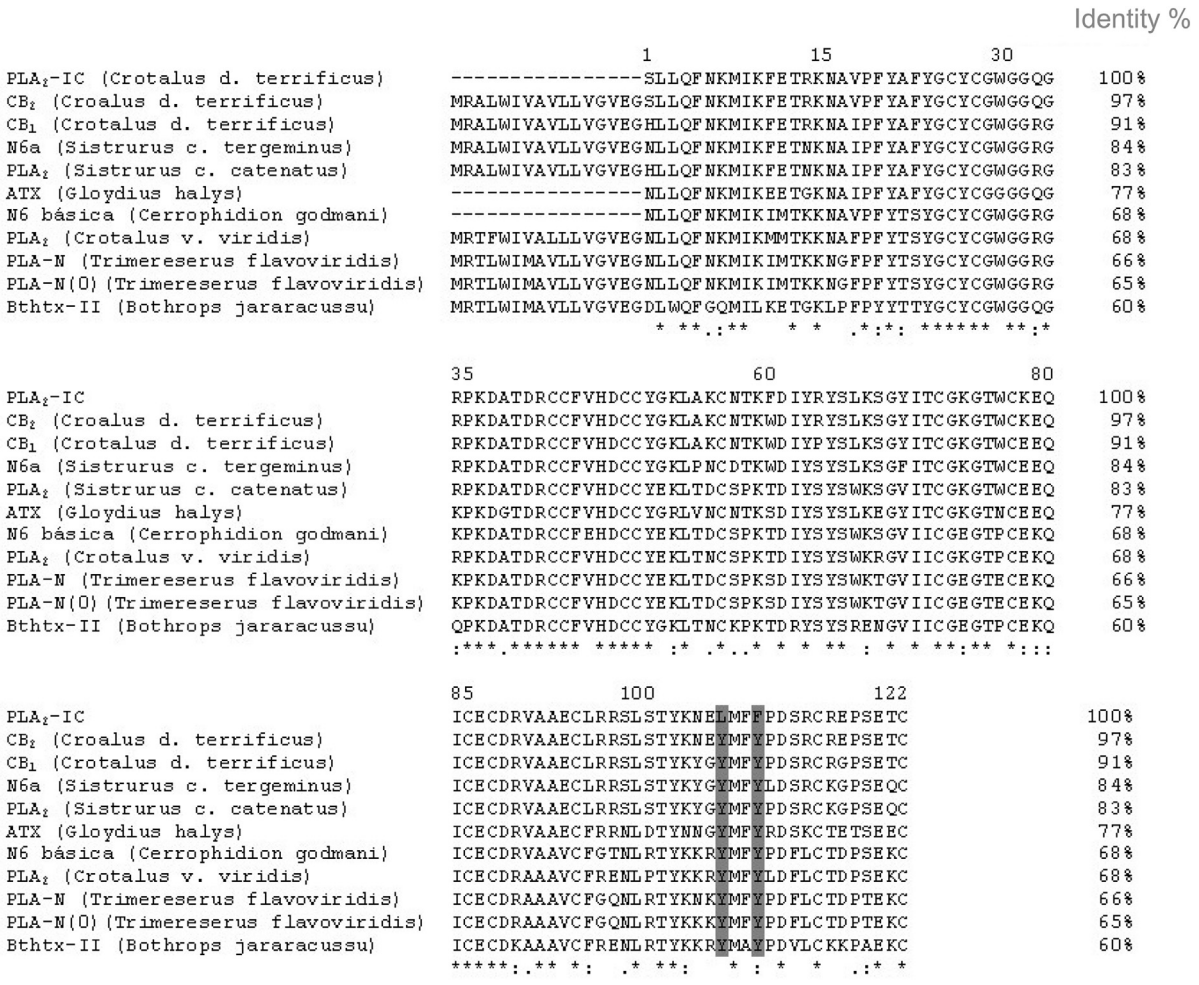

Fig. 4. Comparison between the N-terminal sequences from IC and other snake venom Asp49-PLA_2s. CBc/CB1 isoform (*C. durissus terrificus*, gi: P62022), CBa_2/CB2 isoform (*C. durissus terrificus*, gi:P24027), N6a (*Sistrurus c. tergeminus*, gi:AAR14164), PLA_2 (*Sistrurus c. catenatus*, gi: ABY77918), ATX (*Gloydius halys*, gi:P14421), N6 basic PLA_2 (*Cerrophidion godmani*, gi: AAR14161), PLA_2 (*Crotalus v. viridis*, gi: AAQ13337), PLA-N (*Trimereserus flavoviridis*, gi: Q805A2.2), PLA-N (0) (*Trimereserus flavoviridis*, gi: BAC56893), BthTX-1 (*B. jararacussu*, gi: P45881). Residues in brown correspond to substitutions in the IC C-terminal sequence.

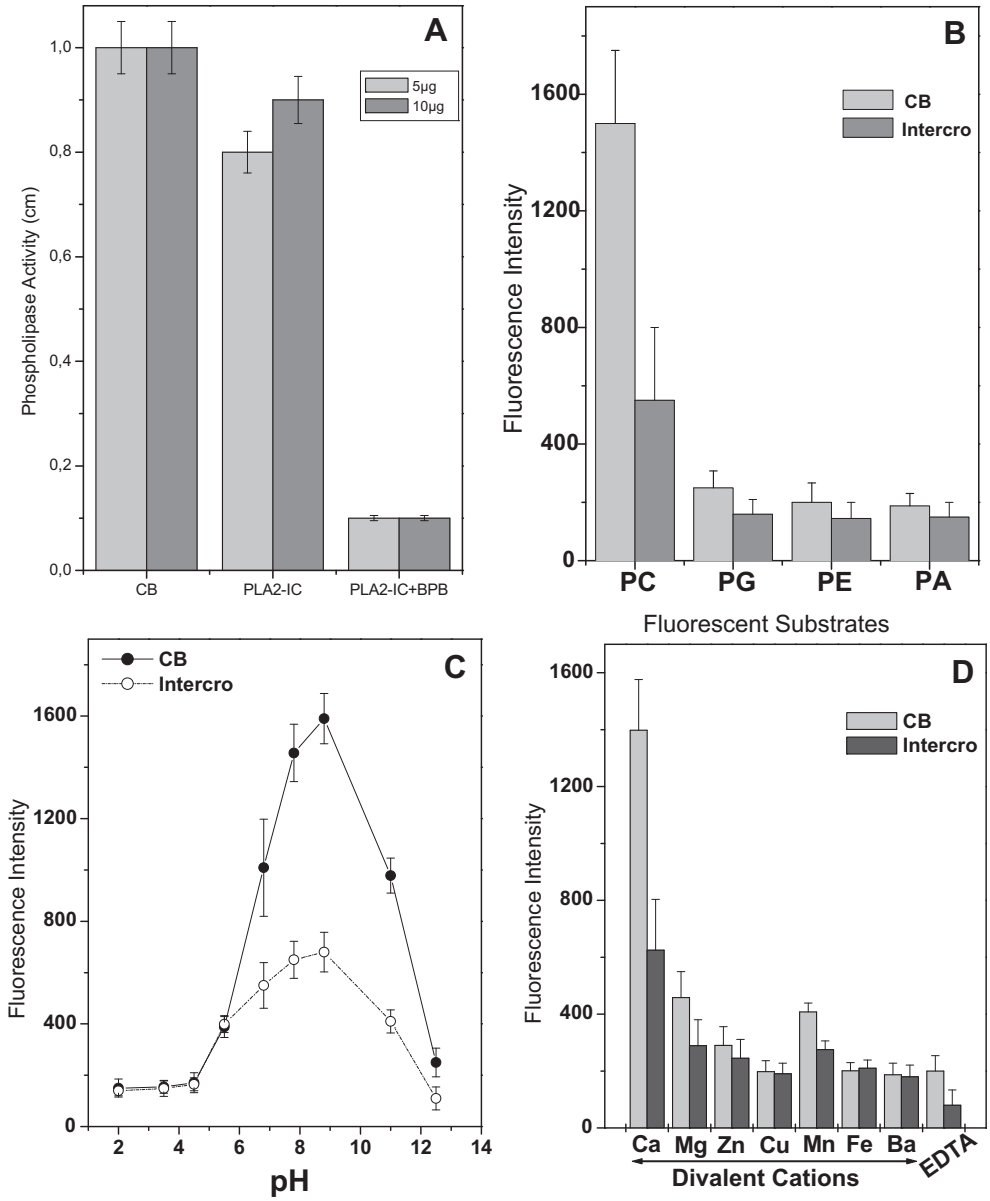

Fig. 5. (A) PLA_2 activity upon egg yolk of CB, IC and IC + pBPB (5 and 10 µg); (B) hydrolysis of different fluorescent substrates (5 mM) by CB and IC (45 µg/mL); (C) influence of pH on the hydrolysis of NBD-PC by CB and IC (45 µg); (D) effect of divalent cations (8 mM) on the hydrolysis of NBD-PC (5 mM) by CB and IC (45 µg/mL), in the absence or presence of 20 mM EDTA. Results expressed in mean ± SD ($n = 3$).

r.m.s.d. (root mean square deviation) was approximately 2 Å. Furthermore, the comparison of the average backbone atom r.m.s.d. between the final 12.5 ns and the previous 12.5 ns of MD simulation showed a difference close to 2.0×10^{-3}, indicating thus a very similar degree of structural variation of the model along the most part of the calculation process.

4. Discussion

4.1. IC presents different biological activities compared with CB isoforms

Snake venom PLA_2s (svPLA_2s) display significant similarities in their tridimensional structure, although they present a wide variety of pharmacological properties. Due to this, these proteins are interesting molecular models for the study of structure and function relationships and physiological/intoxication processes. Therefore, the acquisition of this information could be valuable for the development of new biotechnological products. In this context, the study of IC is potentially important, since from the first report by Laure [16] to date this toxin has not yet been isolated and characterized.

Though at first sight, as suggested by a phylogenetic analysis (Fig. 9B), IC seems to be just a simple CB isoform. The biochemical assays with IC showed that this toxin, like its homologue CB molecules, also presents a considerable His48 dependent PLA_2catalytic activity, as demonstrated by the blockage of the IC catalysis induced by pBPB alkylation. CB and IC were also able to hydrolyze different fluorescent phospholipids, such as PC, PG, PA, and PE, with a higher specificity upon phosphatidylcholine (PC) (Fig. 5). Additionally, the influence of pH and divalent metal ions on both enzymes was similar. In contrast, other assayed cations and EDTA reduced and abolished, respectively, the catalytic activity of the two toxins.

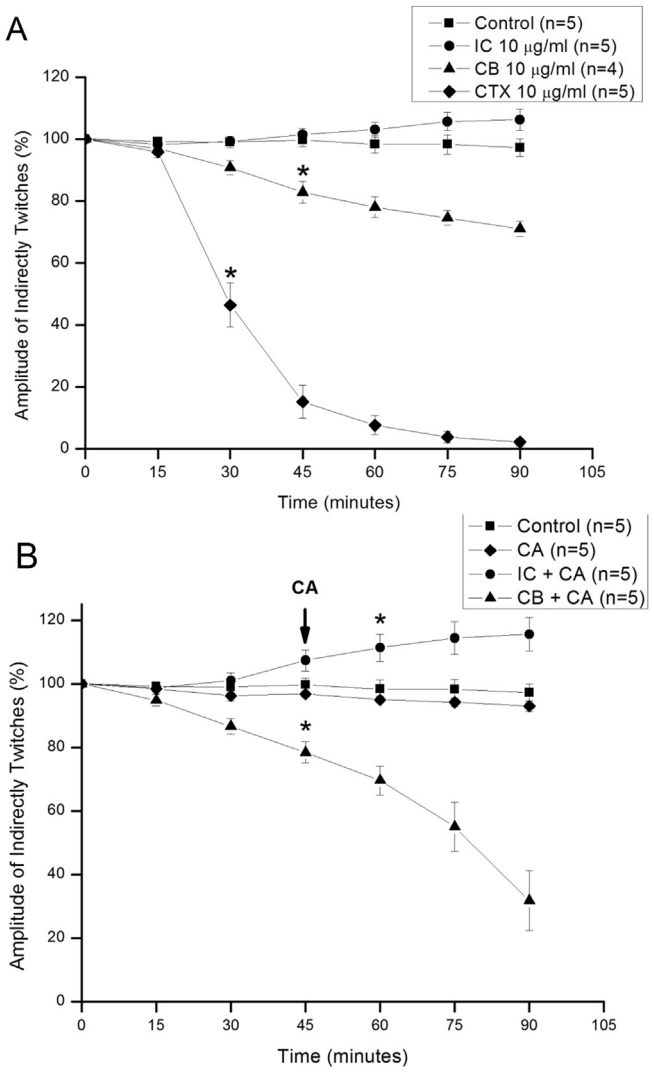

Fig. 6. (A) Effects of Intercro (IC), PLA_2 subunit of crotoxin (CB) and crotoxin (CTX) on indirectly evoked twitches on mice phrenic-diaphragm muscle preparations. (B) Influence of crotapotin subunit of crotoxin (CA) upon the effects of IC and CB. The ordinate represents the % amplitude of indirectly twitches relative to the initial amplitude. The abscissa indicates the time (min) after the addition of substances to the organ bath. Arrow indicates the moment of CA administration. Vertical bars represent mean ± SEM. *Indicates the point from which there are significant differences relative to control ($p < 0.05$).

However, despite the similar CB and IC edema inducing activity, the first toxin was clearly more myotoxic in comparison to the last one (Fig. 7). In addition, differently from the crotoxin complex (CA/CB association) and CB, IC was not able to affect the neuromuscular transmission, indicating that IC presents a distinct pattern of biological activity. Thus, based on these data, it is possible to state that IC is a new toxin, which keeps an enzymatic activity similar to the CB isoforms but shows low myotoxicity and a total absence of neurotoxicity.

4.2. Functional, structural and phylogenetic data indicate a non-association between CA and IC

According to the functional assays, IC together with or without CA did not block the neuromuscular transmission, a typical action of the crotoxin complex and, in a much lower proportion, CB isoforms in the absence of CA (Fig. 6). Considering that the efficiency of the crotoxin complex in produce neurotoxic effect depends on the ability of CA to drive CB to the nerve terminal [40,41], it is possible to hypothesize that the interaction between IC and CA, if exist, isn't able to drive IC to the nerve terminal, as also suggested by the seminal work of Laure [16] and our chromatographic experiments, which showed that at pH 3.5 (and range pH 4.5 at 8.0, Supplemental data), IC was obtained alone and not in a complex form associated with CA, such as observed for crotoxin complex, that is found in a stable complex form in range pH 3.5 at 8.0 (Fig. 1A, Supplemental data). In fact, a structural basis for this supposition could be proposed based on the comparison of IC with the three CB isoforms structurally solved to date (CBa_2, CBb, and CBc) [15,27] and also on a phylogenetic analysis involving this toxin and homologue proteins available in databanks (Table 1).

Despite the presence of highly conserved residues in the N-terminal α-helix h1, active site region, Ca^{2+} binding loop, β-wing, and α-helix h3, there are 11 variable positions between the amino acid sequences of IC and those of CBa_2, CBb and CBc (Fig. 9A). All these positions correspond to amino acid residues probably placed on the IC surface, as indicated by the inspection of the theoretical IC model. This finding points out that these positions may probably reveal some insights into structural features of IC. On this regard, the IC amino acid residues Phe70, Leu117 and Phe120 seem particularly promising to shed some light on these questions, since they are exclusively present in the IC sequence whereas the same positions in the isoforms CBa_2, CBb, and CBc are occupied by the residues Trp70, Tyr117 and Tyr120 (Fig. 9A). Remarkably, Faure et al. [15] have pointed out that CBb His1 and Trp70 are key residues involved in the formation of the heterodimer CA_2/CBb and also in other CA/CB associations. In the CA_2/CBb crystallographic

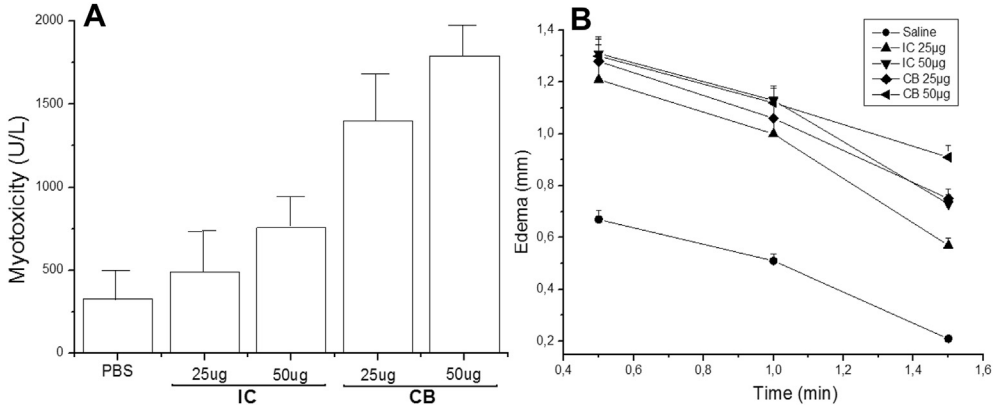

Fig. 7. (A) Myotoxicity induced by IC and CB. (B) Edema induced by CB, IC (25 and 50 μg) in the mouse paw (18–22 g). Results expressed by mean ± SD ($n = 5$).

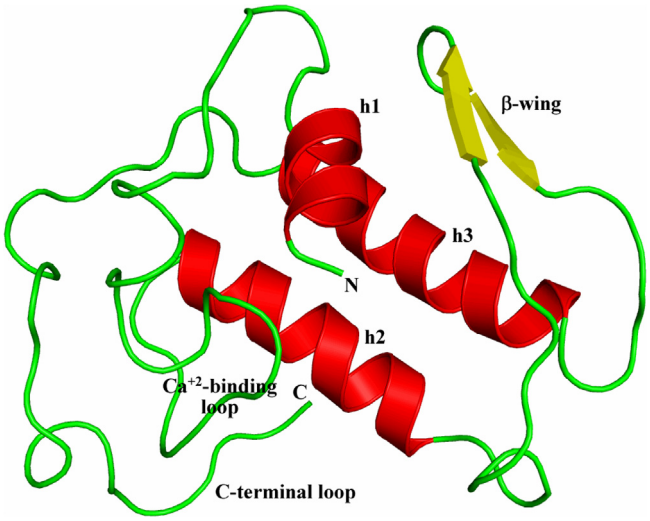

Fig. 8. Cartoon representation of the theoretical IC model, highlighting the secondary structures typically found in group II PLA_2s: N-terminal α-helix (h1); Ca^{2+} binding loop; two antiparallel α-helixes (h2 and h3); two short antiparallel β-ribbons (β-wing), and C-terminal loop. Illustration generated by program PyMOL v.1.3 (The PyMOL Molecular Graphics System, Version 1.3, Schrödinger, LLC).

structure, CBb Trp70 makes 29 interactions shorter than 4.5 Å with residues from CA_2 β-chain (including a stabilizing hydrogen bond with CA_2 Asp89), while CBb His1 is essential to keep, via structural up holding of a neighbor loop (residues 67–71), the appropriate arrangement of the Trp70 side chain. Consequently, based on these structural findings, it is possible to infer that the absence of a neurotoxic active CA/IC complex may be attributed to the presence of IC mutations His → Ser1 and Trp70 → Phe, which probably impairs the formation of a stable CA/IC interface. In addition, Faure et al. [15], based on the CA_2/CBb crystallographic model and CBa_2, CBb, and CBc structural superposition, showed that the positions 1 and 70 are also essential to explain the functional differences between crotoxin classes (class I – high toxicity, low enzymatic activity and higher stability; class II – moderate toxicity, high enzymatic activity and lower stability) [42]. Indeed, residue Ser1 in class II CA/CBa_2 crotoxin complex weakens the stability and toxicity of this heterodimer due to the significant conformational change (around 9.2 Å) of the CBb loop 67–71.

As mentioned above, the orientation change of this CBb loop leads to the displacement of Trp70, preventing the formation of the stabilizing hydrogen bond with CA_2 Asp89. These experimental results allow the proposal of a stability level of the crotoxin complexes, where (i) the heterodimers with residues CB His1 and Trp70 are more stable (CBb and CBc isoforms), (ii) the heterodimers with residues Ser1 and Trp70 present a transitional stability (CBa_2 isoform), and (iii) the heterodimer is not formed when only the residue Ser1 is present (IC, with the mutations His → Ser1 and Trp70 → Phe). Furthermore, analysis of a phylogenetic tree with IC and several homologue $svPLA_2$s proteins strengths the feasibility of this stability-based hierarchy hypothesis of the Crotoxin heterodimers, since IC and CBa_2 are phylogenetically closer when compared with the isoforms CBb and CBc (Fig. 9B). Thus, the gene duplications responsible for the emergence of the CB isoforms

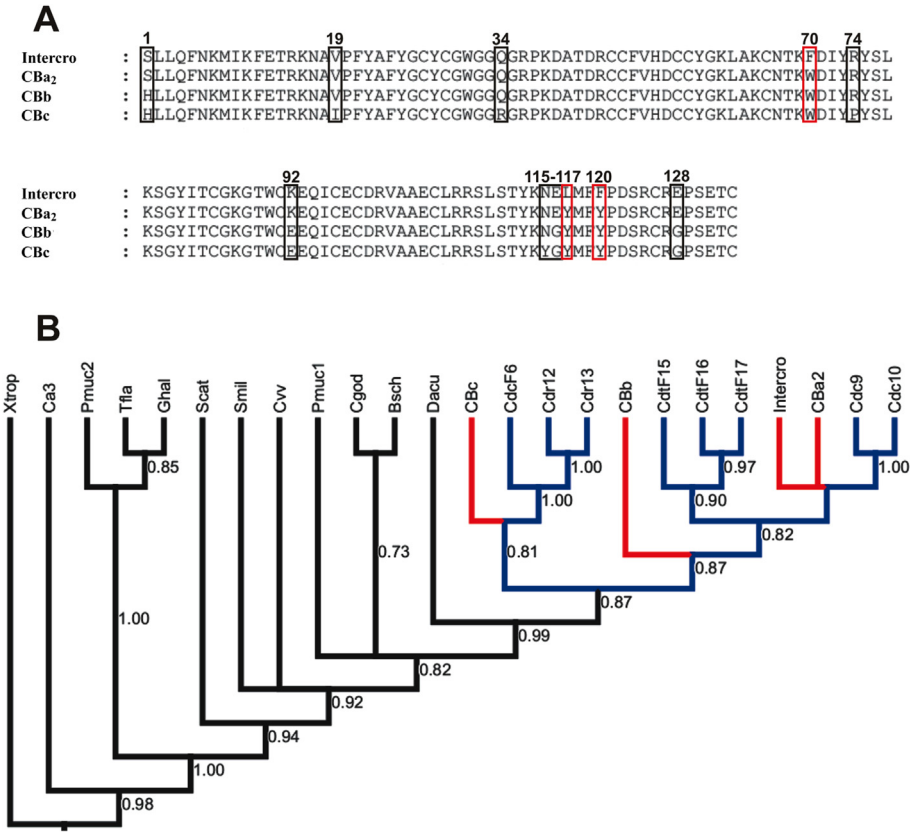

Fig. 9. (A) Sequence alignment highlighting the 11 variable positions between IC and the three CB isoforms structurally solved to date (CBa_2, CBb, and CBc); (B) Bayesian phylogenetic tree with the IC sequence and homologous sequences generated by the program MrBayes v.3.1.2. IC and the structure-solved CBa_2, CBb, and CBc are nested in the red branches and the remaining CB isoforms are nested in the blue branches. The hypothetical phospholipase A_2 LOCI100145401 from *Xenopus tropicalis* was defined as outgroup. Phylogenetic tree was drawn with the program Mesquite v.2.75 (Maddison and Maddinson, 2011).

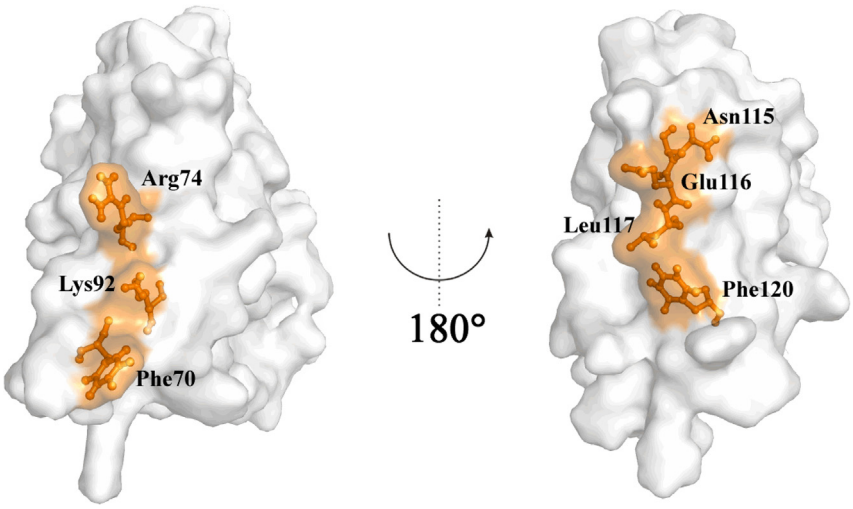

Fig. 10. Clusters on the surface of the IC MD model where the three exclusive IC amino acid residues (Phe70, Leu117, and Phe120) are sited. These IC clusters, which are placed in opposite sides of the molecule and are formed, respectively, by three (Phe70, Arg74, and Lys92) and four (Asn115, Glu116, Leu117, and Phe120) amino acid residues, could be important for substrate/molecular recognition and/or oligomerization. Illustration generated by program PyMOL v.1.3 (The PyMOL Molecular Graphics System, Version 1.3, Schrödinger, LLC).

seem to signal an evolutionary tendency to the formation of lesser stable CA/CB associations, culminating in a CA-independent toxin with possible toxic effects not related to the typical CB neurotoxic activity. This apparent paradox, which in principle seems to point to the selection of isoforms with a moderate toxicity in detriment of higher toxic complexes, may be explained by the increased toxin diversity, an efficient evolutionary strategy in the biochemical arms race between venomous animals and their prey.

Another intriguing issue linked to the questions discussed above is related to the oligomerization of this toxin. As shown in Fig. 1C, IC forms molecular aggregates as observed for others PLA_2s [43], and it is mainly dimeric (M_r ~28,000); after reduction by mercaptoethanol the toxin is monomeric (M_r ~14,600), as reinforced by mass spectrometry (M_r ~14,284). Dynamic light scattering (DLS) experiments confirmed this molecule, in a 3.0 mg mL^{-1}concentration, is dimeric at 298 K. This finding suggests that the molecular diversity is also improved by an extra level of oligomerization, with the potential formation of new molecular-recognition sites not present in the isolated monomers.

A similar possibility was raised by Marchi-Salvador et al. [27], who described the tetrameric crystal structure formed by the combination of two CBa_2/CBb dimers. In this work, the authors hypothesized that the isoforms CBb and CBa_2 (identified respectively as CB1 and CB2) could associate after CA/CB dissociation in order to generate a quaternary assembly able to identify different substrates and even increase the toxicity of the CB toxins. In fact, analysis of the variable positions on the surface of the theoretical model reveals two IC clusters where the three exclusive IC residues (Phe70, Leu117, and Phe120) are sited. These IC clusters are placed in opposite sides of the molecule and are formed, respectively, by three (Phe70, Arg74, and Lys92) and four (Asn115, Glu116, Leu117, and Phe120) amino acid residues (Fig. 10). Therefore, it is possible to suppose that these regions could be important for the IC biological activities, acting as substrate/molecular recognition regions on the monomeric and dimeric IC molecular forms and/or as oligomerization sites. Furthermore, residue IC Ser1 suggests another hint related to the possible quaternary assembling of this toxin: Marchi-Salvador et al. [27] demonstrated that this residue found in the isoform CBa_2 is essential to the stabilization of the dimeric CBa_2/CBc crystal structure, since it forms two salt bridges with CBc Glu92. Interestingly, the hydrodynamic radii (R_H) of the CBa_2/CBc association and the IC dimeric form are practically identical (2.7 and 2.6 nm, respectively), suggesting that the oligomeric arrangement of both dimers may be very similar. Also, it sounds feasible not only the oligomerization between IC molecules but also the quaternary combination of this toxin with CB isoforms.

In conclusion, in spite of the similarity between IC and the CB isoforms, the results of our analyses indicated that IC is a new snake venom toxin. The biological activities of this molecule still remain not completely understood, but the combination of more functional and structural characterizations could permit the elucidation of this puzzling question in order to verify our hypothesis proposed here.

Acknowledgments

The authors are grateful to Ministry of Science and Technology (MCT), Conselho Nacional de Desenvolvimento Científico e Tecnológico (CNPq), Financiadora de Estudos e Projetos (FINEP), Coordenação de Aperfeiçoamento de Nível Superior (CAPES) – Projeto NanoBiotec, Fundação de Amparo à Pesquisa do Estado de São Paulo (FAPESP), Fundação Carlos Chagas Filho de Amparo à Pesquisa do Estado do Rio de Janeiro (FAPERJ), Rede de Biodiversidade e Biotecnologia da Amazônia Legal (BIONORTE/CNPq/MCT), Instituto Nacional para Pesquisa Translacional em Saúde e Ambiente na Região Amazônica (INCT-INPeTAm/CNPq/MCT), Instituto Nacional para Pesquisa em Toxinas (INCT-Tox), Secretary of Development of Rondonia State (SEPLAN/PRONEX/CNPq) for financial support. This work was authorized by Conselho de Gestão do Patrimônio Genético (CGEN/MMA) under the authorization no. 010627/2011-1.

Appendix A. Supplementary data

Supplementary data related to this article can be found at http://dx.doi.org/10.1016/j.biochi.2013.08.028.

References

[1] E. Valentin, G. Lambeau, What can venom phospholipases A_2 tell us about the functional diversity of mammalian secreted phospholipases A_2? Biochimie 82 (2000) 815–831.
[2] J.M. Gutiérrez, B. Lomonte, G. León, A. Alape-Girón, M. Flores-Díaz, L. Sanz, Y. Angulo, J.J. Calvete, Snake venomics and antivenomics: proteomic tools in

the design and control of antivenoms for the treatment of snakebite envenoming, J. Proteomics 72 (2009) 165–182.
[3] S.K. Pal, A. Gomes, S.C. Dasgupta, A. Gomes, Snake venom as therapeutic agents: from toxin to drug development, Indian J. Exp. Biol. 40 (2002) 1353–1358.
[4] J.J. Calvete, L. Sanz, Y. Angulo, B. Lomonte, J.M. Gutiérrez, Venoms, venomics, antivenomics, FEBS Lett. 583 (2009) 1736–1743.
[5] C. Montecucco, J.M. Gutiérrez, B. Lomonte, Cellular pathology induced by snake venom phospholipase A_2 myotoxins and neurotoxins: common aspects of their mechanisms of action, Cell. Mol. Life Sci. 65 (2008) 2897–2912.
[6] P. Rosenberg, The relationship between enzymatic activity and pharmacological properties of phospholipases, in: J.B. Harris (Ed.), Natural Toxins, Oxford University Press, Oxford, 1986, pp. 129–174.
[7] J.B. Harris, Snake Toxins, Pergamon Press, New York, 1991.
[8] A.M. Soares, M.R.M. Fontes, J.R. Giglio, Phospholipases A_2 myotoxins from *Bothrops* snake venoms: structure–function relationship, Curr. Org. Chem. 8 (2004) 1677–1690.
[9] R.C. De Paula, H.C. Castro, C.R. Rodrigues, P.A. Melo, A.L. Fuly, Structural and pharmacological features of phospholipases A_2 from snake venoms, Protein Pept. Lett. 16 (2009) 899–907.
[10] C.H. Slotta, H. Fraenkel-Conrat, Estudos químicos sobre os venenos ofídicos. Purificação e caracterização do veneno de cobra cascavel, Mem. Inst. Butantan 12 (1938–1939) 505.
[11] S.C. Sampaio, S. Hyslop, M.R.M. Fontes, J. Prado-Franceschi, V.O. Zambelli, A.J. Magro, P. Brigatte, V.P. Gutierrez, Y. Cury, Crotoxin: novel activities for a classic beta-neurotoxin, Toxicon 55 (2010) 1045–1060.
[12] R.A. Hendon, H. Fraenkel-Conrat, Biological roles of the two components of crotoxin, Proc. Natl. Acad. Sci. U. S. A. 68 (1971) 1560–1563.
[13] K. Rubsamen, H. Breithaupt, E. Habermann, Biochemistry and pharmacology of the crotoxin complex.Naunyn-Schmiedebergs, Arch. Pharmacol. 270 (1971) 274–288.
[14] G. Faure, V. Choumet, C. Bouchier, L. Camoin, J.L. Guillaune, B. Maneger, M. Veullhorjne, C. Bon, The origin of the diversity of the crotoxin isoforms in the venom of *Crotalus durissus terrificus*, Eur. J. Biochem. 223 (1994) 161–164.
[15] G. Faure, H. Xu, F.A. Saul, Crystal structure of crotoxin reveals key residues involved in the stability and toxicity of this potent heterodimeric β-neurotoxin, J. Mol. Biol. 412 (2011) 176–191.
[16] C.J. Laure, Die Primarstruktur des crotamins, Hoppe-Zeyller's Z. Phisiol. Chem. Bd. 365 (1975) 213–215.
[17] R.F. Itzhaki, D.M. Gill, A microbiuret method for estimating proteins, Anal. Biochem. 9 (1964) 401–410.
[18] P. Doty, E.P. Geiduschec, in: H. Neurath, K. Bailey (Eds.), The Proteins. I–A, 1953.
[19] U.K. Laemmli, Cleavage of structural proteins during the assembly of the head of bacteriophage T4, Nature 227 (1970) 680–685.
[20] J.M. Gutiérrez, C. Avila, E. Rojas, L. Cerdas, Alternative *in vitro* method for testing the potency of the polyvalent antivenom produced in Costa Rica, Toxicon 26 (1988) 411–413.
[21] R.S. Rodrigues, L.F. Izidoro, S.S. Teixeira, L.B. Silveira, A. Hamaguchi, M.I. Homsi-Brandeburgo, H.S. Selistre-de-Araújo, J.R. Giglio, A.L. Fuly, A.M. Soares, V.M. Rodrigues, Isolation and functional characterization of a new myotoxic acidic phospholipase A_2 from *Bothrops pauloensis* snake venom, Toxicon 50 (2007) 153–165.
[22] A.M. Soares, S.H. Andrião-Escarso, Y. Angulo, B. Lomonte, J.M. Gutiérrez, S. Marangoni, M.H. Toyama, R.K. Arni, J.R. Giglio, Structural and functional characterization of a myotoxin I from *Bothrops moojeni* (caissaca) snake venom, Arch. Biochem. Biophys. 373 (2000) 7–15.
[23] A.S. Schwartz, L. Pachter, Multiple alignment by sequence annealing, Bioinformatics 23 (2007) 24–29.
[24] B. Mau, M. Newton, B. Larget, Bayesian phylogenetic inference via Markov chain Monte Carlo methods, Biometrics 55 (1999) 1–12.
[25] J.P. Huelsenbeck, F. Ronquist, MrBayes: bayesian inference of phylogenetic trees, Bioinformatics 17 (2001) 754–755.
[26] J. Söding, A. Biegert, A.N. Lupas, The HHpred interactive server for protein homology detection and structure prediction, Nucleic Acids Res. 33 (2005) 244–248.
[27] D.P. Marchi-Salvador, L.C. Corrêa, A.J. Magro, C.Z. Oliveira, A.M. Soares, M.R.M. Fontes, Insights into the role of oligomeric state on the biological activities of crotoxin: crystal structure of a tetrameric phospholipases A_2 formed by two isoforms of crotoxin B from *Crotalus durissus terrificus*, Proteins Struct. Funct. Bioinform. 72 (2008) 883–891.
[28] M.A. Marti-Renom, A. Stuart, A. Fiser, R. Sanchez, F. Melo, A. Sali, Comparative protein structure modeling of genes and genomes, Annu. Rev. Biophys. Biomol. Struct. 29 (2000) 291–325.
[29] V.B. Chen, W.B. Arendall III, J.J. Headd, D.A. Keedy, R.M. Immormino, G.J. Kapral, L.W. Murray, J.S. Richardson, D.C. Richardson, MolProbity: all-atom structure validation for macromolecular crystallography, Acta Crystallogr. D66 (2010) 12–21.
[30] M. Wiederstein, M.J. Sippl, ProSA-web: interactive web service for the recognition of errors in three-dimensional structures of proteins, Nucleic Acids Res. 35 (2007) W407–W410.
[31] H.J.C. Berendsen, D. Van Der Spoel, R. Van Drunen, GROMACS: a message-passing parallel molecular dynamics implementation, Comp. Phys. Commun. 91 (1995) 43–56.
[32] B. Hess, D. van der Spoel, E. Lindahl, GROMACS 4: algorithms for highly efficient, load-balanced, and scalable molecular simulation, J. Chem. Theory Comput. 4 (2008) 435–447.
[33] H.J.C. Berendsen, J.P.M. Postma, W.F. Van Gunsteren, J. Hermans, Interaction models for water in relation to protein hydration, in: B. Pullman (Ed.), Intermolecular Forces, D. Reidel Publishing Company, Dordrecht, 1981, pp. 331–342.
[34] C. Oostenbrink, T.A. Soares, N.F.A. Van Der Vegt, W.F. Van Gunsteren, Validation of the 53A6 GROMOS force field, Eur. Biophys. J. 34 (2005) 273–284.
[35] H.J.C. Berendsen, J.P.M. Postma, A. DiNola, J.R. Haak, Molecular dynamics with coupling to an external bath, J. Chem. Phys. 81 (1984) 3684–3690.
[36] A.M. Soares, V.M. Rodrigues, M.I. Homsi-Brandeburgo, M.H. Toyama, F.R. Lombardi, R.K. Arni, J.R. Giglio, A rapid procedure for the isolation of the Lys-49 myotoxin II from *Bothrops moojeni* (caissaca) venom: biochemical characterization, crystallization, myotoxic and edematogenic activities, Toxicon 36 (1998) 503–514.
[37] L.A. Ponce-Soto, P.A. Baldasso, F.F. Romero-Vargas, F.V. Winck, J.C. Novello, S. Marangoni, Biochemical, pharmacological and structural characterization of two PLA_2 isoforms Cdr-12 and Cdr-13 from *Crotalus durissus ruruima* snake venom, Protein J. 26 (2007) 39–49.
[38] F.F. Romero-Vargas, L.A. Ponce-Soto, D. Martins-de-Souza, S. Marangoni, Biological and biochemical characterization of two new PLA_2 isoforms Cdc-9 and Cdc-10 from *Crotalus durissus cumanensis* snake venom, Comp. Biochem. Physiol. C Toxicol. Pharmacol. 151 (2010) 66–74.
[39] D.A. Six, E.A. Dennis, The expanding superfamily of phospholipase A_2 enzymes: classification and characterization, Biochim. Biophys. Acta 1488 (2000) 1–19.
[40] C. Bon, J.P. Changeux, T.W. Jeng, H. Fraenkel-Conrat, Postsynaptic effects of crotoxin and of its isolated subunits, Eur. J. Biochem. 99 (1979) 471–481.
[41] E. Délot, C. Bon, Model for the interaction of crotoxin, a phospholipase A_2 neurotoxin, with presynaptic membranes, Biochemistry 32 (1993) 10708–10713.
[42] G. Faure, A.L. Harvey, E. Thomson, B. Saliou, F. Radvanyi, C. Bon, Comparison of crotoxin isoforms reveals the stability of the complex plays a major role in its pharmacological action, Eur. J. Biochem. 214 (1993) 491–496.
[43] R.K. Arni, R.J. Ward, Phospholipase A_2 – a structural review, Toxicon 34 (1996) 827–841.